*Int. J. Solids Structures* Vol. 29, No. 1, pp. 27–39, 1992
Printed in Great Britain.

0020–7683/92 $3.00 + .00


# THE GROWTH OF PRESSURIZED PLANAR CRACKS BETWEEN BARRIERS

X. Li and L. M. Keer
Department of Civil Engineering, Northwestern University, Evanston, IL 60208, U.S.A.

(*Received* 24 *July* 1990; *in revised form* 28 *January* 1991)

**Abstract**—Bower and Ortiz's finite perturbation method is used to analyze the gradual growth of penny-shaped and half-planar cracks between barriers whose fracture toughness is greater than that of the fracture zone. The breakthrough of a crack front into barriers when the stress intensity factor at some points along the interfaces exceeds the fracture toughness of the barriers is considered and the associated changes in the distribution of stress intensity factor and the pressure on the crack faces is calculated. The results indicate that under constant pressure on crack faces, a bounded crack expands indefinitely while a semi-infinite crack would grow stably.

## INTRODUCTION

The solution of crack growth problems is of practical interest in many fields. For the analysis of the damage mechanism of various structural components, the growth of cracks under varying loads is often a process which has to be taken into account. Hydraulically induced fracturing has been used for years by the oil industry for the secondary recovery of petroleum. This technique is now also applied to some other fields such as geothermal energy extraction and radioactive waste disposal. For successful application to hydraulic fracturing, knowledge about the growth pattern of cracks and the associated variation in hydraulic pressure on the crack faces is required.

When the geometry of cracks and load conditions are given, a variety of well established analytical and numerical methods are available in the literature and can be employed to solve for the stress intensity factor along the crack front. For crack growth problems, however, neither the shape of the crack nor the distribution of stress intensity factor are known *a priori* and can only be determined through the solution procedure.

Murakami and Nemart-Nasser (1983) studied the growth of two adjacent surface cracks. By calculating the stress intensity factor for several assumed crack contours, they discussed the stability of crack growth. The fluctuation in the maximum stress intensity factor in their results indicates that the actual crack front curve in the growth process is somewhere between the assumed contours. Mastrojannis *et al.* (1980) and Lee and Keer (1986) investigated the crack growth induced by hydraulic fracturing. The crack front advance was determined by adopting an *ad hoc* fatigue crack growth law. The normal velocity of propagation of a point on the crack contour was assumed to be proportional to the difference between the stress intensity factor and the local fracture toughness of the material to a certain power. The solution procedure was essentially an iterative process, searching for the actual crack geometry. While the fracture criterion may be satisfied for the final geometry of the crack, at any intermediate status during the iteration it is not, and hence the searching process does not represent the actual process of crack growth.

In recent years Rice (1985, 1987) and Gao and Rice (1986, 1987a,b) have developed a theory for calculating the first order variation in crack opening displacement and stress intensity factor due to small changes in crack geometry. Configurational stabilities of straight half-plane cracks and circular cracks are assessed based on this first order perturbation theory. Gao and Rice (1989) have also analyzed crack trapping by arrays of tough obstacles in a brittle matrix. By comparing numerical results with those obtained by Fares (1989) using the boundary element method, the range of validity of this first order analysis can be judged.

Bower and Ortiz (1990) extended Rice's first order perturbation scheme to arbitrarily large variations of crack geometries. By repeated small perturbations to some initial

geometry, results for cracks of arbitrary shapes can be derived. At each step of the perturbation procedure the stress intensity factor is calculated by using the first order formula. At the same time, the influence function is also updated successively for each perturbed crack contour. Comparison with known analytical solutions shows that the accuracy of results is maintained after some hundreds of steps of perturbations.

Since the method reduces the analysis to evaluating one-dimensional integral equations defined on the crack front, it has certain computational advantages over some other existing numerical techniques, which involve discretization of two-dimensional areas on crack faces. Due to the nature of the small perturbation scheme, this procedure is especially suitable for solving crack growth problems.

In this paper the finite perturbation scheme of Bower and Ortiz is extended to study the gradual growth of planar cracks between barriers with larger fracture toughness, induced by the variation of pressure on the crack faces. At each step the fracture criterion that the stress intensity factor is less than or equal to the local fracture toughness is satisfied along the crack front. When the stress intensity factor at some points along the interfaces exceeds the fracture toughness of the barriers, breakthrough will occur and these points will then be allowed to advance into barriers. Two kinds of initial crack geometry are considered, the penny-shaped circular crack and the semi-infinite crack with straight front. The crack growth is accompanied by variation of the pressure applied on the crack faces, which may increase or decrease depending upon the crack geometry considered.

## FORMULATION

In this section a brief outline of the finite perturbation method will be given. A more detailed derivation of the equations presented here and elaboration of the method are given in the papers of Rice (1985, 1987) and Bower and Ortiz (1990).

Consider a planar crack subjected to loads which induce a distribution of mode I stress intensity factor around the crack front $C$. Suppose that under the load condition the crack front begins to grow. Each point at the crack front advances a distance $\delta a(s)$ along the direction normal to $C$, into a new position on the perturbed crack front $\bar{C}$. Based on the theory of weight functions and the consideration of energy variation, Rice (1985, 1987) derived the following two equations, which enable one to calculate the first order variations $\delta K(t)$ and $\delta D(s,t)$ in stress intensity factor and influence function respectively, resulting from the perturbation of the crack geometry:

$$\delta K(t) = \frac{1}{2\pi}\int_C K(s)D(s,t)\delta a(s)\,\mathrm{d}s \tag{1}$$

$$\delta D(s,t) = \frac{1}{2\pi}\int_C D(s,\lambda)D(\lambda,t)\delta a(\lambda)\,\mathrm{d}\lambda. \tag{2}$$

Equations (1) and (2) are the basic equations of this perturbation method. Equation (1) is used to calculate the stress intensity factor along the crack front when the crack advance $\delta a(s)$ is prescribed. Alternatively, the crack advance can be determined if the change in $K(s)$ is known. In the latter case eqn (1) is viewed as an integral equation for the unknown function $\delta a(s)$. In either case, once the new crack front $\bar{C}$ is determined, eqn (2) is used to update the influence function $D(s,t)$ for $\bar{C}$. This procedure can be repeated for further perturbations of the crack front.

One difficulty associated with the application of eqns (1) and (2) is the strong singularity possessed by the influence function $D(s,t)$. In general, the integral in eqn (1) contains a singularity of order $(t-s)^{-2}$ and is only defined in the principal value sense, if the crack front advance $\delta a(s)$ satisfies certain conditions. However, as shown by Rice (1985, 1987), for cracks under uniform load in a homogeneous, isotropic medium this difficulty can be overcome by applying a translation $\delta \mathbf{x} = \delta a(t)\mathbf{n}(t)$ for eqn (1) and a combination of a self-similar expansion, a translation and a rotation for eqn (2) to $C$ to obtain a reference

configuration $C^{\text{ref}}$. The displacement $\delta a^{\text{ref}}(s)$ from $C^{\text{ref}}$ to the new crack front $\bar{C}$ then satisfies the required conditions. After this regularization, the following equations are derived:

$$\bar{K}(\bar{t}) = K(t) + \frac{1}{2\pi}\int_C K(s)D(s,t)\{\delta a(s) - [\mathbf{n}(s)\cdot\mathbf{n}(t)]\delta a(t)\}\,\mathrm{d}s \tag{3}$$

$$\frac{\Phi(\bar{s},\bar{t})}{S(\bar{t}-\bar{s})} = \frac{\Phi(s,t)}{q^2 S(t-s)} + \frac{1}{2\pi q^3}\int_C \frac{\Phi(s,\lambda)}{S(\lambda-s)}\frac{\Phi(\lambda,t)}{S(\lambda-t)}\delta a^{\text{ref}}(\lambda)\,\mathrm{d}\lambda \tag{4}$$

where $\Phi(s,t)/S(s-t) = D(s,t)$, $\Phi(s,t)$ is a bounded function, $S(s-t) = (c/\pi)^2\sin^2[\pi(t-s)/c]$ for bounded cracks and $S(s,t) = (t-s)^2$ for half-plane cracks.

For the crack growth problem analyzed in this paper, the fracture criterion $K(s) \leqslant K_c(s)$ is used, where $K_c$ is the fracture toughness of the material. The faces of the crack are loaded with a uniform normal pressure $P$, which induces a stress intensity factor $K(s) = P\hat{K}(s)$. With the pressure build-up, the stress intensity factor will increase gradually and eventually will reach the local fracture toughness over some portion of the crack front: $P\hat{K}(s) = K_c$. At this stage any arbitrarily small increase in pressure will force the crack front to advance. The crack front advances to a new position, where the fracture criterion along the crack front is satisfied:

$$K(s) + \delta K(s) \leqslant K_c. \tag{5}$$

From eqn (3), over the portion of the crack front where the equality sign in eqn (5) holds, the following equation can be derived (Bower and Ortiz):

$$\frac{-\delta P}{P}\hat{K}(t) = \frac{1}{2\pi}\int_C \hat{K}(s)D(s,t)\{\delta a(s) - [\mathbf{n}(s)\cdot\mathbf{n}(t)]\delta a(t)\}\,\mathrm{d}s. \tag{6}$$

When the new crack front is determined by solving $\delta a(s)$, eqn (4) is used to update $\Phi(s,t)$. For the new crack front, the analysis described above can then be repeated.

Since the basic equations for the calculation of the variation of $K(s)$ and $D(s,t)$ are accurate only to the first order in $\delta a(s)$, as noted before, each step of the perturbation of the crack front must be kept small enough to ensure the accuracy of the numerical results, and thus a large number of perturbations are required when solving problems involving large deformations of crack geometry. However, for many crack growth problems of interest, this feature of small perturbations is desirable because it allows one to monitor more closely the process of crack growth and the resulting changes in other variables. Since the fracture criterion is satisfied for each perturbation step along the crack front, the perturbation process in this analysis should represent the actual process of crack growth. Moreover, the present analysis removes the necessity to assume some relation between the normal velocity of crack propagation, the stress intensity factor and the crack toughness of the material. The crack front advance is determined naturally in the solution procedure only by the requirement that the fracture criterion be satisfied.

## NUMERICAL SCHEME

The solution procedure begins from some appropriate reference crack geometry, whose distribution of stress intensity factor and influence function are known. Two kinds of initial crack geometries are considered here: the internal circular crack and the half-plane crack.

For these two kinds of cracks subjected to uniform pressure on crack faces,the stress intensity factor is constant along the crack front and is denoted by $K_0$. When the stress intensity factor exceeds the fracture toughness at some points along the crack front, these points will be allowed to advance. The advance $\delta a(s)$ is determined by solving eqn (6) under the restriction that $\delta a(s) = 0$ over the portion of the crack front where the stress intensity factor is less than the local fracture toughness.

For general crack geometries, the integral equation (6) can only be solved by numerical methods. Following Bower and Ortiz, the crack front is divided into $n$ elements with three nodes for each element. The crack front curve over each element is approximated by a parabola through three nodal points. The functions $\Phi$ and $K$ are expressed by their nodal values through piecewise quadratic Lagrange interpolation. To ensure that $\delta a'(s)$ is Hölder continuous, the unknown function $\delta a(s)$ is approximated by Hermitian interpolation based on the nodal values of $\delta a(s)$ and $\delta a'(s)$, $s = s_{2k}$, $k = 0, 1, 2, \ldots, n$.

By the above discretization procedure, eqn (6) is reduced to a set of linear algebraic equations in $\delta a(s_{2i})$ and $\delta a'(s_{2i})$:

$$\frac{-\delta P}{P}\hat{K}(t_j) = \frac{1}{2\pi}\sum_{i=0}^{n}\{w_{2i}(t_j)\delta a(s_{2i}) + \hat{w}_{2i}(t_j)\delta a'(s_{2i})\} - \frac{\delta a(t_j)}{2\pi}\sum_{i=0}^{2n} v_i(t_j)[\mathbf{n}(s_i)\cdot\mathbf{n}(t_j)] \quad (7)$$

where the collocation points $t_j$ are set between nodal points, $s_j < t_j < s_{j+1}$. The integration weights $w_i(t_j)$, $\hat{w}_i(t_j)$ and $v_i(t_j)$ can be calculated explicitly (Bower and Ortiz, 1990). A problem encountered in our calculation of $w_i(t_j)$ and $\hat{w}_i(t_j)$ is that when $|t_j - s|$ is not small the integration

$$I_{jk} = \int_{s_{2k}}^{s_{2k+2}} \sum_{i=2k}^{2k+2} [\gamma(s_i, t_j)\Phi(s_i, t_j)K(s_i)]\frac{L_i(s)H(s, s_{2k}, s_{2k+2})}{(t_j - s)^2}\,\mathrm{d}s \quad (8)$$

may be inaccurate due to the subtraction of large positive and negative numbers. This difficulty may be overcome by changing the integral to

$$I_{jk} = \int_{s_{2k}}^{s_{2k+2}} \sum_{i=2k}^{2k+2} \left[\frac{\lambda_k + t_j - s_i}{t_j - s_i}\right]^2 [\gamma(s_i, t_j)\Phi(s_i, t_j)K(s_i)]\frac{L_i(s)H(s, s_{2k}, s_{2k+2})}{(\lambda_k + t_j - s)^2}\,\mathrm{d}s \quad (9)$$

where $\lambda_k$ is chosen such that $|\lambda_k + t_j - s| < \delta$, $s_{2k} < s < s_{2k+2}$, and where $\delta$ is a small constant being smaller than one.

After solving eqn (10) for $\delta a(s_i)$ and $\delta a'(s_i)$, eqn (4) is used to update $\Phi(s_i, t_j)$ by numerical integration. Equation (4) is derived in a form suitable for numerical evaluation of the principal value integration by Bower and Ortiz (1990). In the numerical evaluation of the integral, the functions $\Phi(s_i, \lambda)\Phi(\lambda, t_j)$ and $G\{\delta a^{\mathrm{ref}}(\lambda)\}$ are approximated by Lagrange interpolation over each element. For the element containing the collocation point $t_j$, $s = t_j$ is purposely chosen as a nodal point for the Lagrange interpolation in order to ensure that as the integration point approaches $t_j$, the numerator of the integrand will tend to zero.

## RESULTS AND DISCUSSION

The perturbation scheme described in the preceding sections is used to analyze two cases: the hydraulically induced penny-shaped crack expansion between barriers and the growth of semi-infinite cracks between barriers. Both problems are of interest in reservoir engineering to aid in the understanding of issues such as the stability of a barrier to breakthrough of a crack, when a layer contained within the barriers is being fractured hydraulically. The actual problems encountered often involve the growth of cracks in layered structures. Due to the constraints imposed by the technique involved the layering is approximated by discontinuities in the fracture toughness.

### *Hydraulically induced penny-shaped crack expansion between barriers*

The initial crack configuration is assumed to be a circle of unit radius in an infinite elastic solid (Fig. 1). The middle (pay) zone and the barrier zone are considered to have the same elastic modulus but differing fracture toughnesses. With steadily increasing pressure on the crack faces, the stress intensity factor along the crack front will increase gradually and eventually reach the critical value, $K_c$, the fracture toughness of the material in the pay zone. If the pressure is further increased by a small amount, the crack front begins to

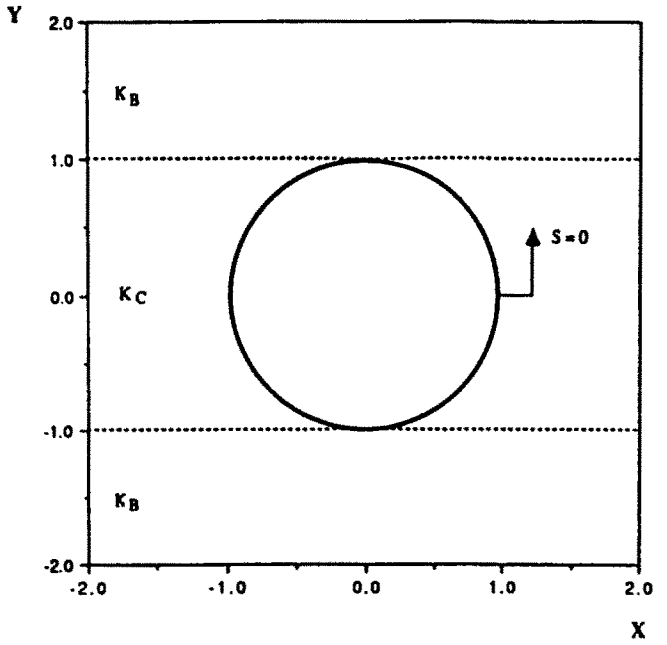


Fig. 1. The geometry of the circular crack between barriers.

advance until the new crack configuration satisfies the fracture criterion $K(s) \leqslant K_c$ along the crack front.

For numerical solution the crack contour is divided into 64 elements. In each step, according to the requirement of small perturbation, $\delta P$ in eqn (15) is chosen such that the maximum crack front displacement, $\delta a_{max}(s) \leqslant 0.01$. Since the fracture toughness in the barriers is considered to be larger than that in the pay zone, the crack expansion is restricted there. The crack expansion is terminated at the interfaces at the first stage of crack growth, when the stress intensity factor along the interfaces does not exceed the fracture toughness of the material in the barrier zone.

Numerical results are shown for this stage of crack growth in Fig. 2a and b. Although the stress intensity factor along the crack front in the middle zone is uniform, $K(s) = K_c$, points on the crack front in the central part of the middle zone tend to advance faster than those points near the interfaces (Fig. 2a), a phenomenon not predictable by the fatigue crack growth law. This result is apparently caused by the presence of the barriers on the upper and lower sides, which hinder the crack front expansion along the vertical direction.

The crack expansion results in a drop in pressure on the crack faces, as shown in Fig. 3. The decline of $P$ is rather sharp at the initial phase. As the crack continues to grow, however, the rate of pressure drop will decrease.

The stress intensity factor at the interfaces increases substantially during the crack growth (Fig. 2b). When it exceeds the fracture toughness of the barrier zones, the crack front will begin to advance into the barriers. Numerical results for this stage of crack growth are shown in Figs 4–6, where $K_c$ and $K_B$ are the fracture toughnesses of the pay zone and the barrier zone, respectively.

In Fig. 4a ($K_B/K_c = 1.257$), it is observed that the growth rate of crack front in the barrier zone is smaller than that in the pay zone. However, the growth rate in the barrier zone is steadily increasing as more and more points along the interfaces, where the stress intensity factor reaches $K_B$ (Fig. 4b), begin to advance.

In the first stage of crack expansion, which is restricted to the pay zone, the rate of pressure drop tends to slow down with crack growth. The breakthrough of the crack front into the barriers, however, will cause a sharp drop in the pressure as can be seen from the curve ($K_B/K_c = 1.257$) in Fig. 3.

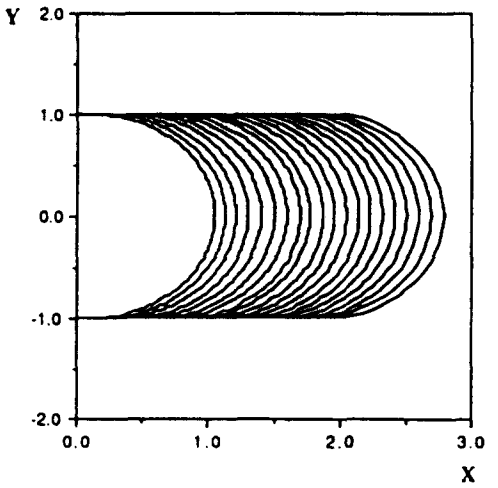


Fig. 2a. The growth of a penny-shaped crack between barriers without breakthrough.

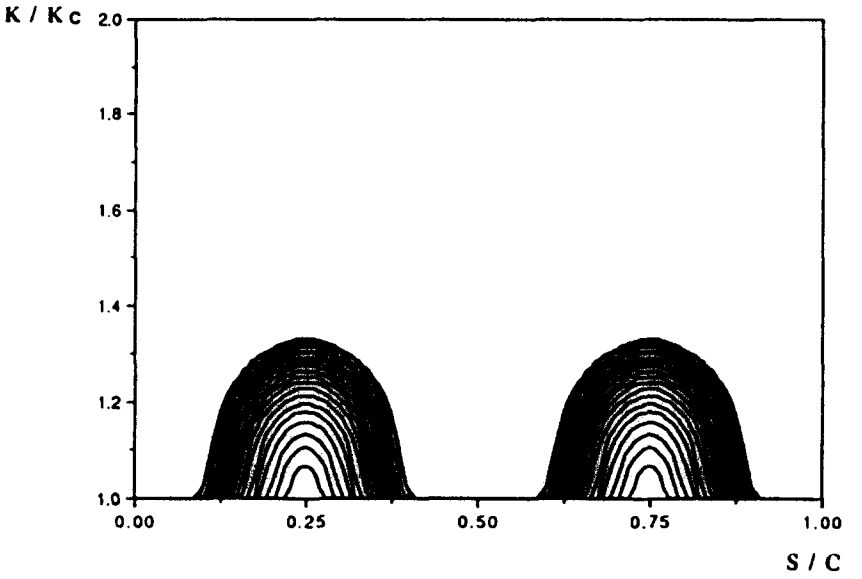


Fig. 2b. The variation of stress intensity factor of a penny-shaped crack during growth without breakthrough.

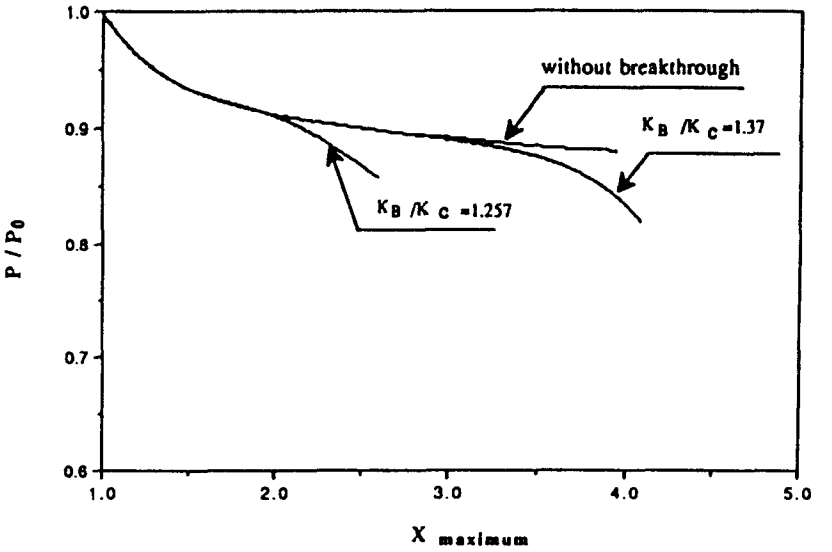


Fig. 3. The variation of pressure on penny-shaped crack faces during crack growth.

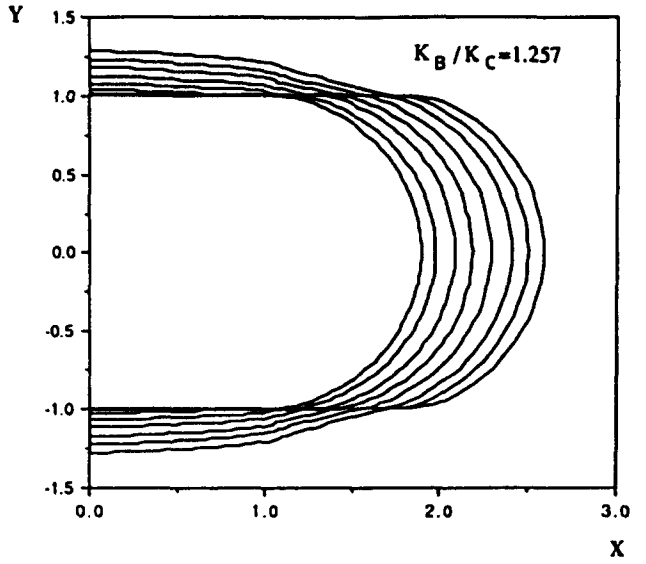


Fig. 4a. The growth of a penny-shaped crack after breakthrough, $K_B/K_C = 1.257$.

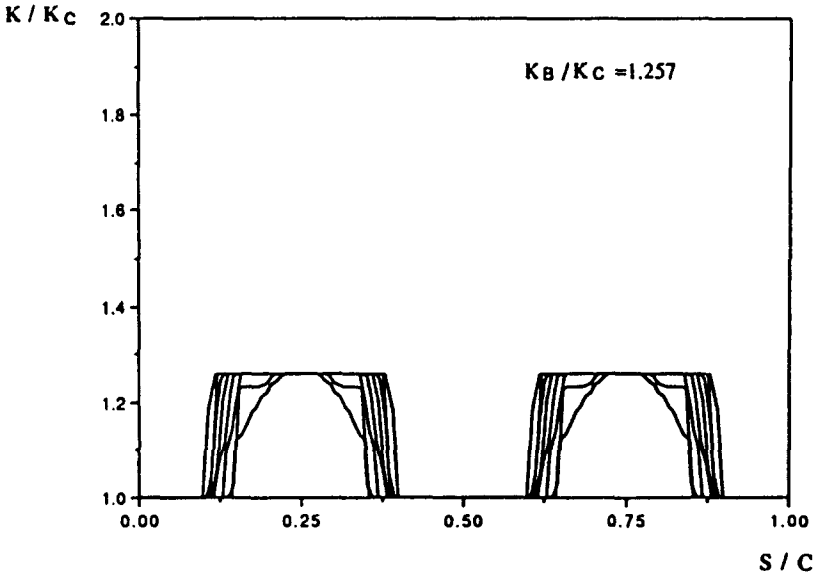


Fig. 4b. The variation of stress intensity factor of a penny-shaped crack after breakthrough, $K_B/K_C = 1.257$.

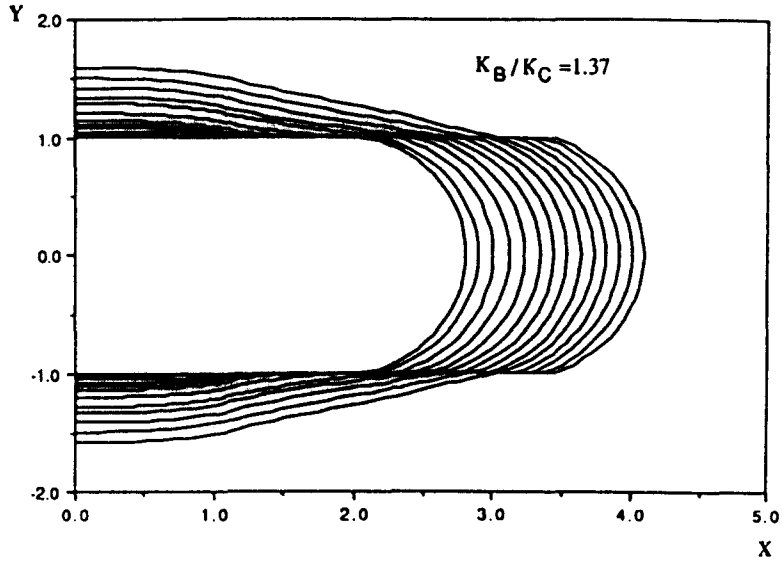


Fig. 5a. The growth of a penny-shaped crack after breakthrough, $K_B/K_C = 1.37$.

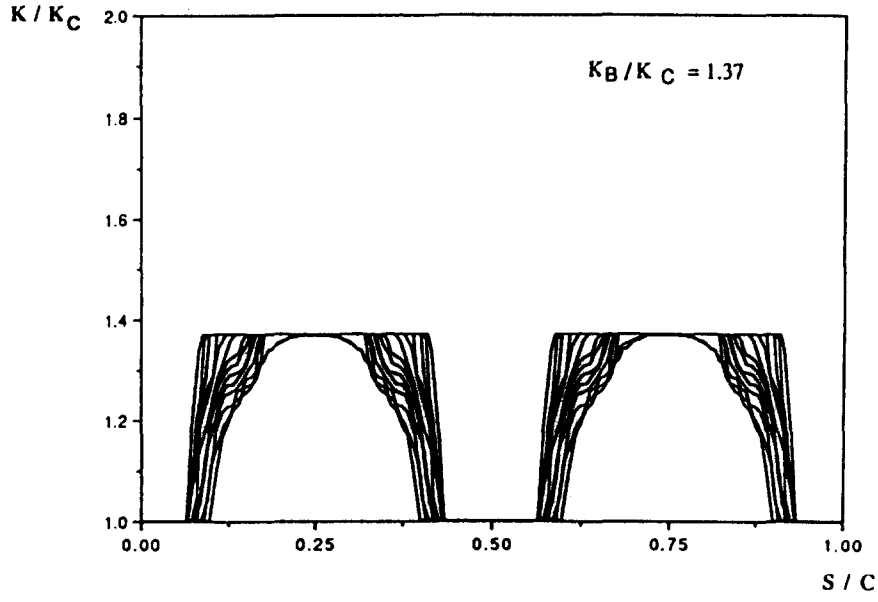


Fig. 5b. The variation of stress intensity factor of a penny-shaped crack after breakthrough, $K_B/K_C = 1.37$.

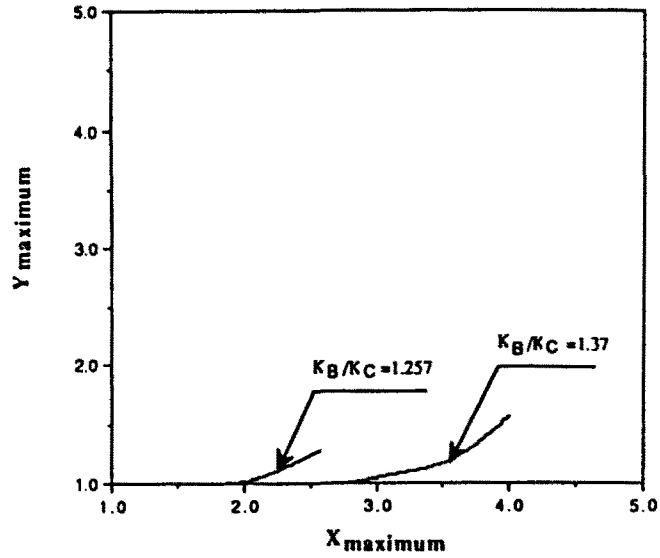


Fig. 6. Comparison of growth rates of penny-shaped cracks along horizontal and vertical directions after breakthrough.

When the ratio $K_B/K_c$ is larger, the breakthrough of crack front into barriers will occur at a later stage of crack growth (Figs 5a and 6). In the initial phase of breakthrough the growth rate of the crack front in the barrier zone is small as is the deviation of pressure drop rate from the curve without breakthrough (Fig. 3). This result occurs since at first only a small part of the whole crack front is involved in the breakthrough process. However, as the crack continues to grow and more and more points along the interface begin to advance, both the crack growth rate in the barrier zone and the pressure drop rate will increase rapidly, as shown in Figs 3 and 6.

The decrease of pressure with the expansion of initially circular cracks may infer that this growth process is unstable. If the pressure remains constant, the advance of the crack front will cause the stress intensity factor to increase and hence the crack will continue to grow in an unbounded manner.

*Growth of semi-infinite cracks between barriers*

The pay zone is located between $-1.0 < y < 1.0$. Only part of the infinite crack front, $-y_0 \leqslant y \leqslant y_0$, is divided into elements and the following assumptions are taken over the remainder of the crack front:

$$\Phi(s, t_j) = \Phi(s_0, t_j), \quad K(s) = K(s_0), \quad \delta a(s) = \delta a(s_0), \quad \text{for} \quad s < s_0,$$

$$\Phi(s, t_j) = \Phi(s_{2n}, t_j), \quad K(s) = K(s_{2n}), \quad \delta a(s) = \delta a(s_{2n}), \quad \text{for} \quad s < s_{2n},$$

where $y_0 = 4.0$ is chosen for the calculation. After the breakthrough of the crack front into barriers, $y_0$ is set to be 6.0. Numerical results show the behavior assumed in the above equations when points approach $s_0$ and $s_{2n}$. In each step of the perturbation $\delta a_{max}(s)$ is restricted to be less than 0.01. The two sharp corners on the crack contour at $x = 0.0$, $y = \pm 1.0$ are smoothed by fitting a parabola through the neighboring nodal points, which is believed not to affect the overall behavior of crack growth.

The growth of the crack front, which is restricted to the pay zone, is shown in Fig. 7a. In the growth process the initially straight crack front between barriers gradually deforms to curves with increasing curvatures. As in the case of circular cracks, points in the central part of the pay zone tend to advance faster than those near the interfaces. The stress intensity factors along the interfaces and in the barriers increase during the crack growth (Fig. 7b) and reach their peak value at the two corners on the crack contour. The variation

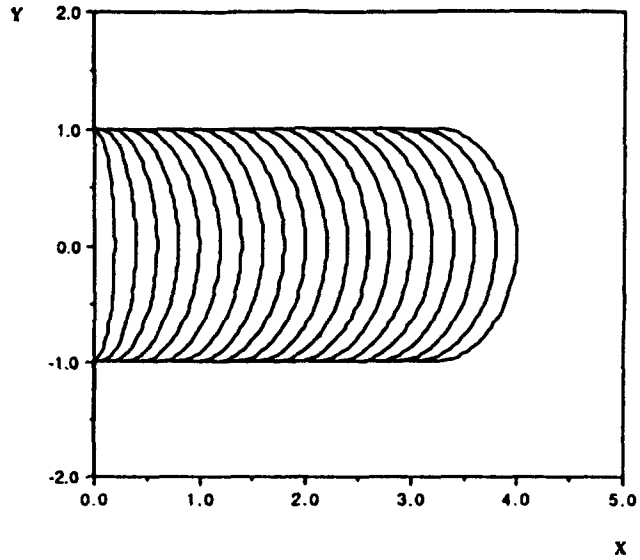


Fig. 7a. The growth of a half-plane crack between barriers without breakthrough.

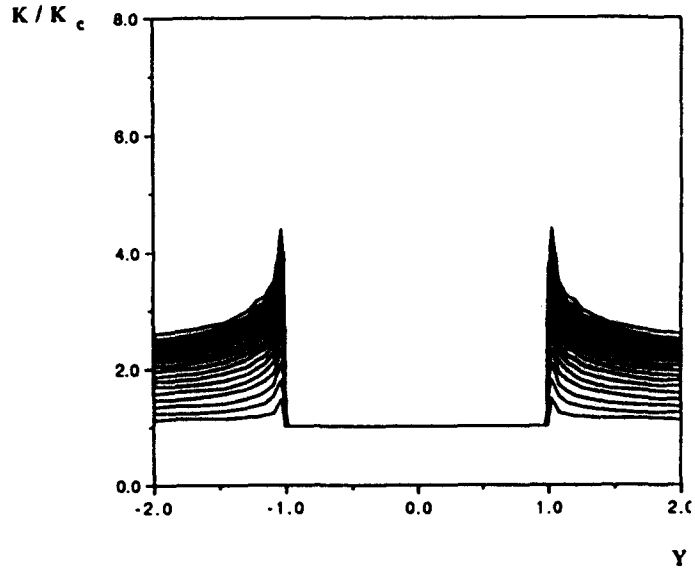


Fig. 7b. The variation of stress intensity factor of a half-plane crack during growth without breakthrough.

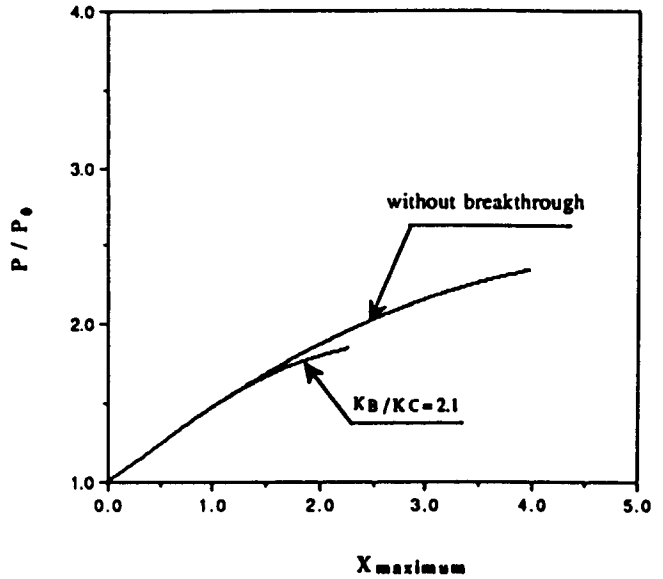


Fig. 8. The variation of pressure on half-plane crack faces during crack growth.

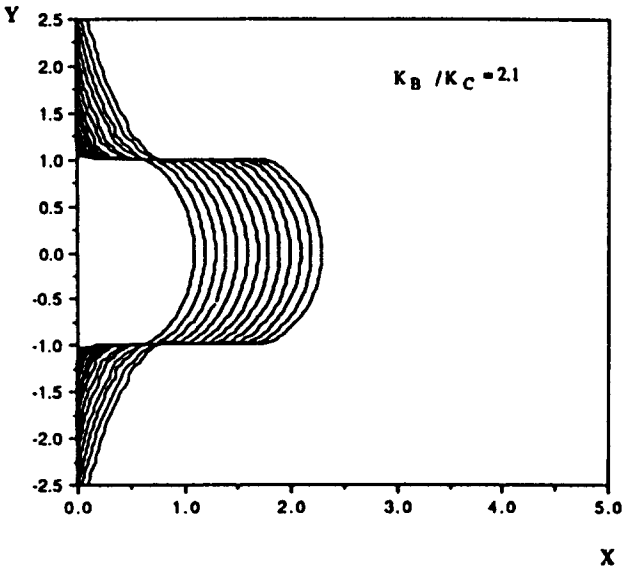


Fig. 9. The growth of a half-plane crack after breakthrough, $K_B/K_C = 2.1$.

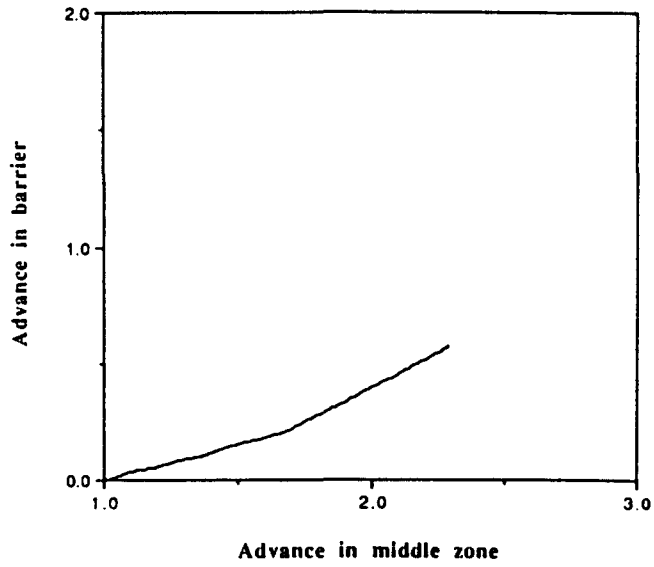


Fig. 10. Comparison of growth rates of half-plane cracks in different zones after breakthrough.

of pressure on the crack faces is shown in Fig. 8. In contrast to the case of bounded cracks, the pressure increases with crack advance and indicates stable crack growth. When the pressure does not increase, the crack will cease to grow.

The breakthrough of the crack front into barriers first occurs at the two corners, where the maximum stress intensity factor reaches the fracture toughness of the barriers. The growth of the crack front after breakthrough is shown in Fig. 9. The comparison of crack growth rates in different zones is made by comparing the advance of the center point in the pay zone and that of the corner points ($x = 0.0, y = \pm 1.0$) (Fig. 10). Figures 9 and 10 show that at first the rate of breakthrough is small. When an increasing number of points are involved along the crack front in the barrier and along the interfaces, the growth rate of the crack front in the barriers will accelerate, causing further breakthrough. The effect of the breakthrough on the variation of pressure on the crack faces is shown in Fig. 8. Only after a large section of the crack front begins to advance into the barriers are appreciable changes in the pressure variation observed.

As shown in the two cases presented here of penny-shaped and half-plane crack growth between barriers, the finite perturbation method is especially suitable for solving crack growth problems, due to its small perturbation feature. One limitation of the application of this procedure at present is that the elastic moduli for the different zones are required to be the same, and the pressure on the crack surfaces must be uniform, which are essential for the regularization of the strongly singular integral in the basic equations. Whether this perturbation method can be extended to solve truly layered medium problems is not clear at present.

*Acknowledgements*—The authors are grateful to Amoco Production Company for the support of this research and particularly to Drs Z. A. Moschovidis and R. W. Veatch for their help and encouragement.

## REFERENCES

Bower, A. F. and Ortiz, M. (1990). Solution of three dimensional crack problems by a finite perturbation method. *J. Mech. Phys. Solids* **38**, 443–480.

Fares, N. (1989). Crack fronts trapped by arrays of obstacles: numerical solutions based on surface integral representations. *J. Appl. Mech.* **56**, 837–843.

Gao, H. and Rice, J. R. (1986). Shear stress intensity factors for a planar crack with slightly curved front. *J. Appl. Mech.* **53**, 774–778.

Gao, H. and Rice, J. R. (1987a). Somewhat circular tensile cracks. *Int. J. Fracture* **33**, 155–174.

Gao, H. and Rice, J. R. (1987b). Nearly circular connections of elastic half spaces. *J. Appl. Mech.* **54**, 627–634.

Gao, H. and Rice, J. R. (1989). A first-order perturbation analysis of crack trapping by arrays of obstacles. *J. Appl. Mech.* **56**, 828–836.

Lee, J. C. and Keer, L. M. (1986). Study of three-dimensional crack terminating at an interface. *J. Appl. Mech.* **53**, 311–316.

Mastrojannis, E. N., Keer, L. M. and Mura, T. (1980). Growth of planar cracks induced by hydraulic fracturing. *Int. J. Numer. Meth. Engng* **15**, 41–54.

Murakami, Y. and Nemart-Nasser, S. (1983). Growth and stability of interacting surface flows of arbitrary shape. *Engng Fracture Mech.* **17**, 193–210.

Rice, J. R. (1985). First order variation in elastic fields due to variation in location of a planar crack front. *J. Appl. Mech.* **52**, 571–579.

Rice, J. R. (1987). Weight function theory for three-dimensional elastic crack analysis. In *Fracture Mechanics: Perspectives and Directions, Twentieth Symposium* (Edited by R. P. Wei and R. P. Gangloff), ASTM-STP-1020, pp. 29–57. American Society for Testing and Materials, Philadelphia.